VNU Journal of Science: Mathematics – Physics, Vol. 34, No. 4 (2018) 44-61

VNU Journal of Science: Mathematics - Physics

Journal homepage: https://js.vnu.edu.vn/MaP

Data Processing Methods for Deep Level Transients Measurement

Pham Quoc Trieu, Hoang Nam Nhat*

Faculty of Physics, VNU University of Science, 334 Nguyen Trai, Thanh Xuan, Hanoi, Vietnam

Received 17 December 2018
Revised 20 December 2018; Accepted 22 December 2018

Abstract: The year 2019 marks 45 years in the development of Deep Level Transient Spectroscopy (DLTS) - the signal processing method for determination of overlapping deep levels in semiconductors. From its introduction in 1974 by David Lang (D.V. Lang, *J. Appl. Phys*. 45, 1974, p.3023) to this date the DLTS method has undergone many changes and modifications: some were purely theoretical speculations, some were to also include new experimental arrangement and technique. This paper provides almost complete review on DLTS, focusing on the main three approaches widely used today. We also summarize the development of this method in the Faculty of Physics, VNU University of Science.

Keywords:

1. Introduction

The existence of the deep levels transient is important phenomenon in semiconductor physics. The characterization of the deep traps faced many difficulties until 1974 when Lang has introduced a spectroscopic method called the Deep Level Transient Spectroscopy (DLTS) [1]. This method allows to detect with appropriate accuracy the existence of overlapping transients cast in the form of the capacitance dependence on time $C(t) = \Delta C e^{-e_n t}$ (Fig.1). The basic physical parameters of the traps such as the activation energy, capture cross-section and concentration can be determined by this technique. The Lang's method has been widely utilized today as a standard tool, although it is known to have several limitations, such as a slow run and low resolution.

To extract the trap parameters from the exponential decays, Lang has introduced a *signal form* of $S(T)=C(t_1)-C(t_2)$ which is technically realized using a double boxcar circuit, which monitors the capacitance transients at two different times. This function S(T) has a desirable property that it shows

*Corresponding author. Tel.: 84-913097735.
Email: namnhat@gmail.com
https//doi.org/ 10.25073/2588-1124/vnumap.4308

maximal gain at certain temperature related to the double boxcar rate windows setting. So by scanning the S(T) over temperature several times one can obtain the functional dependence of emission factor on temperature *e=f(T)* and can construct the Arhenius plot ln(e/T^2) versus 1000/T for the determination of trap parameters (Fig.2). The key element in this technique is thus the determination of the temperature dependence *e=f(T).*

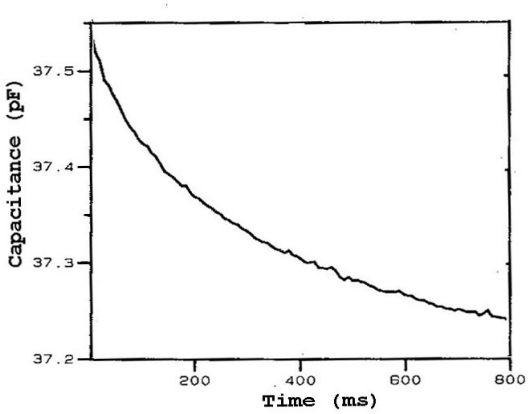

Fig.1. A typical capacitance transient.

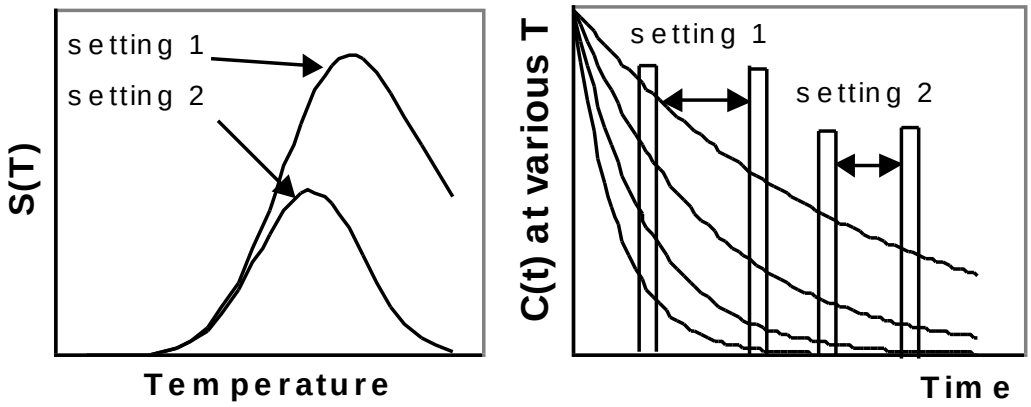

Fig.2. Lang's method scans S(T)=C(t_1)–C(t_2) for various t_1 and t_2 settings and draws the temperature dependence of S(T). The maximum determine the temperatures T of the emission factor e_{max} set forth by the rate windows.

Up to now, many attempts have been made in this field to improve the DLTS method. Among the techniques that have been reported [2-14] (the list is certainly not complete), there are two that attracted general attention (and realization on practice): *the Fourier and the Laplace technique*. These are both transformation methods manipulating with the whole range of measured data, usually containing digitally recorded 512 or 1024 points. Recall that the classical S(T) uses only 2 points and throws the rest away, the Fourier and the Laplace signal forms transform all data and show more sensitive peak structure of the gain, but since they do not involve any rate window the exact emission factor at the maximal gain can not be calculated in advance. The correspondence of the peaks and the deep centers appears in these cases somehow subtle and arbitrary.

2. Lang's signal form

A common feature of all spectroscopic methods is the presentation of the analytic algorithm converting a set of capacitance transients *C(t)*, each of them has been recorded at some preset temperature T, into the specific values of certain analytic functions f_n(T), showing the peak structures according to T. The f_n(T) need to have two important properties: (1) they are *spectroscopic* in the context that each of the peaks in f_n(T) can be associated with one specific deep center and (2) they are *linear*, i.e. the Arhenius plot [ln(e/T^2) versus 1000/T] transformation of the maxima of arbitrarily chosen peak is linear. The functions f_n(T) represent an algorithm and usually a method is named after f_n(T). Hereinafter the f_n(T) are referred to as a *signal form*. For short we may remove the index *n* denoting the time-settings and use *f*(T) instead of f_n(T).

The different signal forms involve the different number of measured data and have the different ability in separation of overlapping deep centers. The classical Lang's signal form, for example, involves only 2 points in the whole transient, whereas the Fourier and the Laplace signal forms are composed principally of whole transients. There is not known any other spectroscopic signal form than the above three until the intervention of [15].

The dependence of the capacitance transient *C(t)* on time *t* is considered in general case as:

$$C(t) = C_0 + \sum \Delta C_i e^{-e_i t} \tag{1}$$

where C_0 is $C(t=\infty)$, $\Delta C=\sum\Delta C_i = C(t=0)–C_0$ and *i* denotes the number of present deep traps.

With respect to a normalized capacitance given as $C_n(t)=(C(t)–C_0)/\Delta C$, and denote $t_1=t–d$, $t_2=t+d$, we redefine the Lang's signal for this general case:

$$S(T) = C_n(t-d) - C_n(t+d) = \sum (\Delta C_i / \Delta C)[e^{-e_i(t-d)} - e^{-e_i(t+d)}] \tag{2}$$

Suppose that the traps are independent and not overlapping each other (they are far from each from other in temperature scale), one may differentiate this signal according to some emission factor e_i, leaving the other ones zeroed, to determine the signal maximal gain in the given temperature range. We modify the result from [1] with respect to the variables *t* and *d* mentioned above:

$$e_{max} = ln[(t+d)/(t–d)]/2d \tag{3}$$

This relation shows that by fixing the rate windows (by *t* and *d*) one also selects the emission factor to which the Lang's signal reacts mostly when it scans through a given temperature range. With the increase of temperature the trap begins to release electrons and it releases mostly when the emission factor is high enough, raising the Lang's signal to maximum. But when the trap becomes blank, the emission process slows down resulting in the drop of Lang's signal. This intuitive understanding of the emission process - although not fully correct, offers a certain physical meaning to the Lang's signal and persuades a belief that it really depicts the physical traps.

3. Fourier DLTS

The pre-historical idea to solve (1) to find an optimal set of { $\tau_i=1/e_i$, c_0 and c_i} has involved a least square refinement and this has been unsuccessful due to the occurrence of many false extremes. After Lang's intervention, in 1988, Weiss and Kassing have introduced a method called Fourier DLTS described as follows [4]. In general, the DLTS is an integral method since it does not measure directly C(t) but a correlation integral signal R(t) with some periodical filter *f*(t) having period T_w:

$$R(t,T) = \frac{1}{T_w}\int_0^{T_w} f(t)C(t,T)dt \tag{4}$$

This integral passes a maximum at certain temperature T when $\tau_m(T)$ is equal to some value preset by filter *f(t)* (usually call rate-windows). By scanning T in a wide range one may find all possible $\tau_m(T)$ because each of $\tau_m(T)$ has its characteristic spectrum. The advantage of this method is that it need not to record all spectrum *C(t, T)* but only those values of integral *R(t, T)* so the data are not large and the processing is fast. However, the most disadvantage is that many important information containing in *C(t, T)* are not taken into account, so the final resolution is limited.

Recall that a differentiable continuous real and periodical function *c(t)* having period T_w (i.e. $c(t) = c(t+nT_w)$ with all $n=0,1,2...$) could be decomposed into a Fourier series:

$$c(t) = \frac{a_0}{2} + \sum_{n=1}^{\infty}\left[a_n \cos(\frac{2\pi}{T_w}nt) + b_n \sin(\frac{2\pi}{T_w}nt)\right] \tag{5}$$

a_n , b_n are to be called the Fourier coefficients. Because the Fourier series is orthogonal, the coefficients a_n , b_n can be determined by multiplying them with *c(t)* and then integrate. Only the integrals with indexes $k \neq n$ are non-zero. We have the inverse transformation:

$$a_n = \frac{2}{T_w}\int_0^{T_w} c(t)\cos(\frac{2\pi}{T_w}nt)dt \tag{6}$$

$$b_n = \frac{2}{T_w}\int_0^{T_w} c(t)\sin(\frac{2\pi}{T_w}nt)dt \tag{7}$$

In case the *c(t)* is a complex function, the complex coefficients c_n are defined as:

$$c_n = \frac{1}{T_w}\int_0^{T_w} c(t)e^{-i\frac{2\pi}{T_w}nt}dt \tag{8}$$

And there is a relation between c_n and a_n, b_n:

$$c_n = \frac{1}{2}(a_n - ib_n) \tag{9}$$

For the discrete Fourier analysis, *c(t)* has only N particular values $c(t_k)$, k=0,1,...,N in a period T_w, the integral (8) becomes:

$$F_n = \sum_{k=0}^{N} c(t_k)e^{-i2\pi n\frac{k}{N}} \tag{10}$$

And there is an empirical dependence between the coefficients F_n and their complex counterparts c_n:

$$F_n = Nc_n^D \tag{11}$$

where *D* is an empirical real constant. This formulae is of great importance for the Weiss and Kassing method because it allows to calculate c_n on the basis of N measurements $c(t_k)$.

Now look at the integral output $R(t) = \frac{1}{T_w}\int_0^{T_w} f(t)C(t)dt$ of the signal *C(t)* and we see that:

- the integral output *R(t)* plays the role of the Fourier coefficients c_n;

- the filter *f(t)* has the form $e^{-i\frac{2\pi}{T_w}nt}$ with period T_w.

With this intuition, the involving of Fourier series in DLTS becomes clear.

The basic procedure is:

a) at some specific T, measure N values of $C(t_k)$ at various times $t_k = k\Delta\tau$, $\kappa = 0, 1, ..., N-1$. The period of *C(t)* will be $T_w = N\Delta t$. Now to find $R(t_k)$ for each $C(t_k)$.

b) suppose that *c(t)* follows the exponential law so *c(t)* is a real function; let the filter *f(t)* be $e^{-i\frac{2\pi}{T_w}nt}$ we calculate the Fourier coefficient a_n , b_n and c_n.

c) now suppose $C(t_k) = c(t_k)$ and we calculate F_n and c_n according to (11) and find the experimental values of a_n and b_n

d) by comparing the theoretical and experimental values a_n and b_n one can find τ at T and trap concentration N_T.

e) now by repeating steps (a), (c) and (d) one can find all possible $\tau(T)$. At the final, one builds the Arhenius plots and determines the activation energy E_T.

The Fourier method requires only one temperature scan, the time τ can be determined directly from the experimental coefficients a_n and b_n measured at each T. In the Lang's approach, one must first fix the rate-windows then scan T and in the Fourier DLTS, one first fix T then scan all rate-windows (512 or 1024 measurements) to find τ.

Suppose we have one trap center emitted according to the exponential law:

$$C(t) = B + Ae^{-\frac{t+t_0}{\tau}} \tag{12}$$

The Fourier coefficients were determined as:

$$a_0 = \frac{2A}{T_w}e^{-\frac{t_0}{\tau}}\left[1-e^{-\frac{T_w}{\tau}}\right]\tau + 2B \tag{13}$$

$$a_n = \frac{2A}{T_w}e^{-\frac{t_0}{\tau}}\left[1-e^{-\frac{T_w}{\tau}}\right]\frac{1/\tau}{1/\tau^2 + n^2\left(2\pi/T_w\right)^2} \tag{14}$$

$$b_n = \frac{2A}{T_w}e^{-\frac{t_0}{\tau}}\left[1-e^{-\frac{T_w}{\tau}}\right]\frac{n2\pi/T_w}{1/\tau^2 + n^2\left(2\pi/T_w\right)^2} \tag{15}$$

So we have:

$$A = \frac{T_w}{2}b_n e^{\frac{t_0}{\tau}}\left[1-e^{-\frac{T_w}{\tau}}\right]^{-1}\frac{1/\tau^2 + n^2\left(2\pi/T_w\right)^2}{n2\pi/T_w} \tag{16}$$

By dividing a_n and b_n for each other, we have several ways to calculate τ:

$$\tau(a_n, a_k) = \frac{T_w}{2\pi}\sqrt{\frac{a_n - a_k}{k^2 a_k - n^2 a_n}} \tag{17}$$

$$\tau(b_n, b_k) = \frac{T_w}{2\pi}\sqrt{\frac{kb_n - nb_k}{k^2 nb_k - n^2 kb_n}} \tag{18}$$

$$\tau(a_n, b_n) = \frac{T_w}{2\pi n}\left[\frac{b_n}{a_n}\right] \tag{19}$$

In the Fourier DLTS we use mostly $\tau(a_1, a_2)$, $\tau(b_1, b_2)$, $\tau(a_1, b_1)$ and $\tau(a_2, b_2)$. In these 4 values, the $\tau(a_1, b_1)$ is usually most correct. With $n=1$ we have a simple relation between a_1, a_2, b_1 and b_2. This relation can be used to check whether or not the measured coefficients $(a_1, a_2, b_1, b_2)_{MEAS}$ do follow the exponential law of emission:

$$\frac{b_1}{a_1}\frac{a_2}{b_2} = \frac{1}{2} \tag{20}$$

If (20) does not hold so the emission is probably caused by overlapping centers.

4. Reference levels in Lang's signal form

One thing that seems either unobserved or attracted no considerable attention from the Lang's time is that the relation (3) used to obtain the e_{max} almost equals $1/t$ numerically. Using the Euler number definition formula $\lim_{n\to\infty}(1+1/n)^n = e$ one can without difficulty prove that $ln[(t+d)/(t-d)]/2d$ really converges to $1/t$ when $d \to 0$. Giving the fact that $ln[(t+d)/(t-d)]/2d \sim 1/t$, the e_{max} always corresponds to $C_n(t)=e^{-1}$ (e is Euler number). This special feature of the classical double boxcar technique is illustrated in Fig.3, where one can see that the e_{max} occurs exactly when $C_n(t)$ passes through the cross-point of the gate central position t and the line $C_n=e^{-1}$. This means that despite of the variation in the rate window positions, the only area of importance was $C_n(t)=e^{-1}$. The evident consequence follows immediately that to detect the functional dependence of the emission factor on the temperature $e_i=f(T)$ one simply check the cross-points of $C_n(t)$ and $C_n=e^{-1}$ to obtain directly the value of emission factor ($e_i=1/t$) corresponding to the given temperature T. For this reason we call $C_n=e^{-1}$ the *reference level* of the signal form S(T). It is a great advantage for the signal form to possess the reference level since this means that $e=f(T)$ can be derived directly from its reference level.

Although the Lang's signal only approaches this reference level in a limit case when the gate width $2d$ is infinitesimally small, there is a lot of other signal forms, as discussed in the next section, which have exact reference level. The importance of reference levels follows from the fact that they lead to an understanding of the algebraic structure of the exponential decays in general and of the capacitance transient in particular. We now introduce the so-called *Lang's signal class* and derive the algebraic structure for this class.

Consider the moving of gate from t to $t'=at$, for a is a positive real number. Since e_{max} depends inversely on t it follows that the emission factor $e_i(t)$ detected on the basis of $e_{max}(t)$ changes as: $e_i(t') = e_i(at) = 1/at = (1/a)e_i(t)$. The transient associated with this $e_i(t')$ will have at time t the value equal to the value of the transient associated with $e_i(t)$ at time t/a:

$$e^{-e_i(t')t} = e^{-e_i(t)t/a} = C_n(t/a) = [C_n(t)]^{1/a}$$

So we can construct a *modified Lang's signal*, to be called a signal of *order a* as follows:

$$S(T)^{[a]} = C_n(t-d)^{1/a} - C_n(t+d)^{1/a} \quad (21)$$

which still has a central position at *t* but produces a maximal output along the reference level $C_n = e^{-a}$ (e=2.718282). Of course, the classical Lang's signal S(T) is of order 1: $S(T)^{[1]}$. With all possible *a*, the system $S(T)^{[a]}$ forms a class of signals - the *Lang's signal class*. The fact that the e_{max} of $S(T)^{[a]}$ really converts to a/t when $d \to 0$ can also be observed by differentiating $S(T)^{[a]}$ according to e_i (leaving all other $e_{j\neq i} = 0$) and set it to 0. The result is: $e_{max}(S(T)^{[a]}) = a\ ln[(t+d)/(t-d)]/2d = ae_{max}(S(T)^{[1]}) = a/t$. When $a<1$, the $S(T)^{[a]}$ reaches $C_n = e^{-a}$ at lower T and when $a>1$ it catches $C_n = e^{-a}$ at higher T in comparison with S(T).

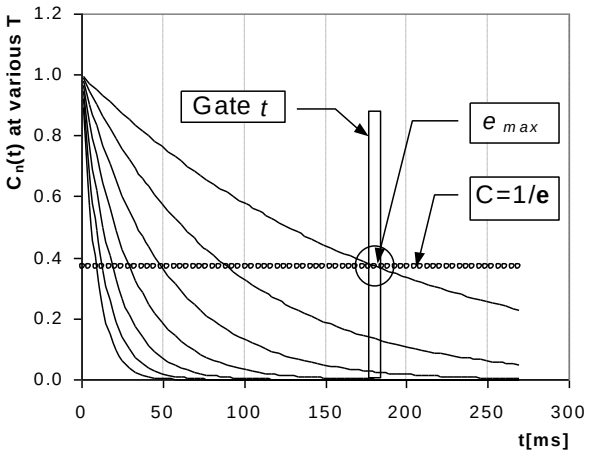

Fig.3. The special feature of the double boxcar technique: the rate window [*t–d, t+d*] shows maximum according to T when the $C_n(t)$ decreases through the area $C_n(t) \sim 1/e = 0.368$.

This signal class associates each point *X* in the plane [$y=C_n(t)$, $x=t$] with some horizontal reference level line $y=e^{-a}$ and the vertical line $x=t$, so that *X* lies in the intersect between these two lines. Each point *X* thus determines a unique emission factor $e_i=a/t$. It is naturally to unify *X* with e_i and write $e_i=e_i(a,t)$. From the analysis above it is obvious that:

$$e_i(a,t) = ae_i(1,t) = e_i(1,t/a) \quad (22)$$

$$e_i(a,t)^n = a^n e_i(1,t)^n = a^n e_i(1,t^n) = e_i(a^n,t^n) = e_i(1,(t/a)^n)$$

This tells us about the equivalence of all reference levels in the signal processing system using a double boxcar technique. The following relations come straightforward.

$$\lambda[e_i(a,t)+e_i(b,t)] = \lambda e_i(a,t)+\lambda e_i(b,t) =$$
$$= \lambda a e_i(1,t)+\lambda b e_i(1,t) = \lambda(a+b)e_i(1,t) = e_i(\lambda(a+b),t) \quad (23)$$

$$[e_i(a,t^n) \times e_i(b,t^m)]^\lambda = e_i(a,t^n)^\lambda \times e_i(b,t^m)^\lambda =$$
$$= a^\lambda e_i(1,t)^{n\lambda} \times b^\lambda e_i(1,t)^{m\lambda} = (ab)^\lambda e_i(1,t)^{\lambda(n+m)} =$$
$$= e_i((ab)^\lambda, t^{\lambda(n+m)}) \quad (24)$$

One may notice that they follow a linear algebra on $\Re^2$.

5. The signal classes and forms

There is an important property of the Lang's signal form: it shows certain separability when the different traps overlap. The signal that is worth to use in practice should be both spectroscopic and resoluble. Up to now, the only spectroscopic signals that brought better resolution were from the transformation of the whole transient. These signals, however, do not possess the reference levels and their algebraic structures are quite different.

This section describes two classes of the signal forms, which we call here the Gaussian and the Poisson class (to the later one the Lang's class $S(T)^{[a]}$ reduces as a special case), possessing the same algebraic structure of the reference levels as the Lang's signal form and also fulfilling the requirement of being resoluble and spectroscopic. The fact that there may exist other spectroscopic signals than the Lang's one can be intuitively recognized from the temperature dependence of $C(t)$ (Fig.4). The simplest way how to create a peak-shape function from the $C(t)=f(T)$ is to either differentiate $C(t)$ according to T (or done by Lang, by substracting $C(t_2)$ from $C(t_2)$, which evidently reduces to the differentiation when the $C(t)$-s become infinitesimally close). These classes are summarized in the Table 1, where the last column shows the estimation for maximal pseudo-random noise level (in % of the maximal signal) that does not disturb their e_{max} more than 5% from the correct value.

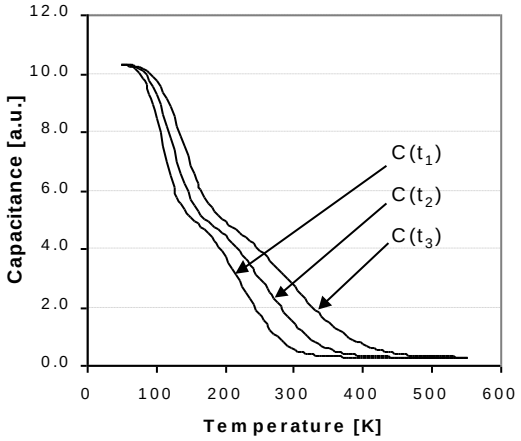

Fig.4. The development of capacitance at three successive times for the Lang's *n*-GaAs example with two traps E=0.44eV and 0.75eV.

In general, the signal classes can be classified into two different groups. The 1st is the *finite element group*, consisting of the classes with signals formed from the finite number of $C(t)$. The 2nd is the *infinite element group* consisting of the classes with signals formed from the infinite number of $C(t)$. This classification can be extended to cover also the 3rd class of signal forms, which deal with the non-analytic algorithms, that is the *fractal group*. Principally, any non-analytic algorithm $F(t,T,C(t,T))$ taking $C(t)$, t, T as the inputs and outputs the peaks can be considered as the signal form if it satisfies the conditions for the signal forms. The study on the 2nd and 3rd groups will be presented elsewhere.

The signal forms are composing from one single $C(t)$ or from a finite number of $C(t_i)$. The Lang's class is a special case where the number of $C(t_i)$ is 2. It is worth to adopt the following notation. According to the number of $C(t_i)$ they consist of the signal form is called the unitary or binary signal form.

Among the unitary signal forms, the Poisson ones - derived from the Poisson distribution function, deserve most attention since they provide sharp peak and their resistibility to noise is high. The Gaussian forms also possess good peak structure but they seem more sensitive to noise. Both these two classes are of e^{-a} reference level class with $e_{max}=a/t$. Fig.5 compares some of them with the classic Lang's form which belongs to the middle quality signals. The Lang's signal form, workable in the interference of 1-1.5% noise, is the best form among the binary ones but is comparable to the Gaussian forms (1.5%) and is worse than the Poisson forms (3-5%).

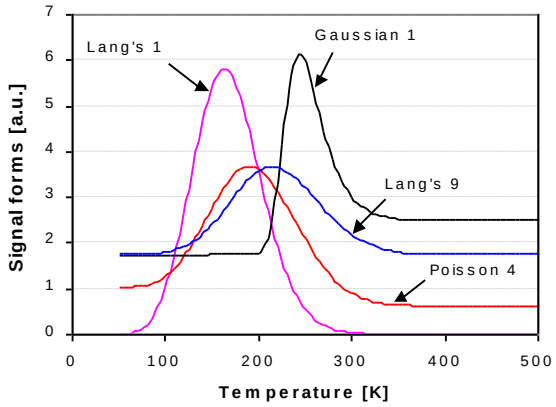

Fig.5. Comparison of some selected signal forms to the classical Lang's S(T) form for a sample with one trap E=0.44eV.

A common feature of the finite element forms is that they all have e^{-a} reference level with a preset. The e_{max} depends only on t and is always a/t. This enables the straightforward construction of the functional dependence $e=f(T)$: at each T when the $C(t)$ is recorded, the time t where $C(t)$ crosses the horizontal line $C=e^{-a}$ determines $e(T)=a/t$. So the repeated scanning of $C(t)$ over the whole temperature range as for the classical DLTS is not needed. The use of the unitary signal forms even makes the measurement process more faster in one aspect that we don't need to scan the whole time t and can set focus onto the specific area. This topic is however the subject of the further study. The existence of the unitary signal forms itself is a surprising fact. Fig.5 illustrates the use of the Gaussian signal form to determinate the traps in the Lang's example n-GaAs.

Table 1. The finit element signal classes: signal forms, their e_{max} and reference levels

Class		Signal forms	e_{max}	Reference level	Max noise
Gauss (unitary)	1	$\beta C(t) - C(t)^{\alpha}$ $e^{[\beta C(t) - C(t)^{\alpha}]}$ usually β =5-10	for α=2, e_{max}= (1/t)ln[2ΔC/(β−2C₀)]	e^{-a}, a= ln[2ΔC/(β−2C₀)]	1.5-2%
	2	$C(t)e^{\beta C(t) - C(t)^{\alpha}}$	for α=2, e_{max}= (1/t)ln[2ΔC/(1+β−2C₀)]	e^{-a}, a= ln[2ΔC/(1+β−2C₀)]	1.5-2%
	3	$ke^{-(C(t)-\mu)^2/2\sigma^2}$ usually μ~1, $2\sigma^2$ = 0.2 k only scales the graph	e_{max}= (1/t)ln[ΔC/(μ−C₀)]	e^{-a}, a= ln[ΔC/(μ−C₀)]	1.0-1.5%

Poisson (unitary)	4	$-C(t)\ln[\alpha C(t)]$ for $0<\alpha<1$, usually $\alpha=0.2$	$e_{max}= (1/t)\ln[\alpha\Delta C/(e^{-1}-\alpha C_0)]$	e^{-a}, $a= \ln[\alpha\Delta C/(e^{-1}-\alpha C_0)]$	3-5%
	5	$C(t)^{\beta}\lambda^{-\alpha C(t)}$ for $\lambda>1$, usually $\lambda=2$	$e_{max}= (1/t)\ln[\Delta C\ln\lambda/(1-C_0\ln\lambda)]$	e^{-a}, $a= \ln[\Delta C\ln\lambda/(1-C_0\ln\lambda)]$	3-5%
Lang (binary)	6	$C_n(t_1)^{1/a}-C_n(t_2)^{1/a}$ need normalized $C_n(t)$ but not for a=1	$e_{max}=a\ln(t_1/t_2)/(t_1-t_2)\sim a/t$	e^{-a}	1-1.5%
	7	$C(t_1)^n/C(t_2)^n$ usually n=1 or 2	for $t_2=2t_1$: $e_{max}=(1/t)\ln(1+\sqrt{1+\Delta C/C_0})$	e^{-a}, $a=\ln(1+\sqrt{1+\Delta C/C_0})$	0.5%
	8	$\alpha\Delta C-(C(t_1)+1/C(t_2))$ can not be used with the normalized $C_n(t)$	for $t_2=t_1=t$ (unitar signal): $e_{max}=-(1/t)\ln(-1+\sqrt{1+1/C_0^2})$	e^{-a} $a=-\ln(-1+\sqrt{1+1/C_0^2})$	1-1.3%
	9	$C_n(t_2)\ln C_n(t_1)-C_n(t_1)\ln C_n(t_2)$ need normalized $C_n(t)$	estimation for $t_2=2t_1$: $e_{max}=1.21188215/t$	e^{-a}, $a=1.21188215$	1-1.3%

6. Averaging functions

6.1. Time averaging functions: the correlation of signals at fixed T

Taking correlations at fixed `T` *de facto* means averaging signal according to time `t`. At fixed temperature the development of signal after a time `t` wholly depends on emission constant e_n and has simple exponential form $e^{-e_n t}$. Let λ be a period width. We will integrate through the whole period.

Cross-correlation of $C_n(t)$ and $1/C_n(t)$

$$R(\tau)=\frac{1}{\lambda}\int_{-\lambda/2}^{\lambda/2}\frac{e^{-e_n t}}{e^{-e_n(t-\tau)}}dt=e^{-e_n\tau}\Rightarrow -\frac{1}{\tau}Ln(R(\tau))=e_n \text{ (for all T)} \quad (25)$$

Autocorrelation of L(t)

$$R(\tau)=\frac{1}{\lambda}\int_{-\lambda/2}^{\lambda/2}(-e_n t)(-e_n t+e_n\tau)dt=\frac{(e_n\lambda)^2}{12} \quad (26)$$

Autocorrelation of -L(t)/t

$$R(\tau)=\frac{1}{\lambda}\int_{-\lambda/2}^{\lambda/2}\left(\frac{-e_n t}{t}\right)\left(\frac{-e_n t+e_n\tau}{t-\tau}\right)dt=e_n^2 \quad (27)$$

One may also check that a cross-correlation of $L(t)^{-1/t}$ and $1/L(t)^{-1/t}$ is always 1.

$$R(\tau)=\frac{1}{\lambda}\int_{-\lambda/2}^{\lambda/2}\left(\frac{-e_n t}{t}\right)\left(\frac{t-\tau}{-e_n t+e_n\tau}\right)dt=1 \quad (28)$$

This relation is extremely useful for checking whether or not the emission follows the exponential law and to indicate the existence of the overlapping centers.

6.2. Temperature averaging functions: the correlation of signals at fixed time

This class of correlation functions illustrates the averaging process according to temperature T, i.e. the process of filtering the temperature noise. Write $C_n(T) = e^{-t\rho T^2 e^{-\omega/T}}$, $L(T)^{-1/t} = \rho T^2 e^{-\omega/T}$ and put $M(T) = Ln[-L(T)^{-1/t}] = Ln\rho + 2LnT - \omega/T$. The correlation is considered within one segment of T so we integrate from T_1 to T_2. Let $\Delta T = T_2 - T_1$.

Cross-correlation between M(T) and 1/M(T)

$$R(\tau) = \frac{1}{\Delta T}\int_{T_1}^{T_2}\left(\rho T^2 e^{-\frac{\omega}{T}}\right)\left(\rho (T-\tau)^2 e^{-\frac{\omega}{(T-\tau)}}\right)dT = \frac{1}{\Delta T}\int_{T_1}^{T_2}\left(\frac{T}{T-\tau}\right)^2\left(e^{-\left(\frac{\omega}{T}-\frac{\omega}{T-\tau}\right)}\right)dT \tag{29}$$

Substitute $x = 1/T$, $x_1 = 1/T_1$, $x_2 = 1/T_2$ and $\Delta x = x_2 - x_1$. Put $A = (1/\Delta x)\,Ln(x_1/x_2)$, $B = 1/(x_1 x_2)$ we have after solving (29):

$$\omega = \frac{1}{\sigma} Ln\left[\frac{1 + 2\sigma A + \sigma^2 B}{R(\sigma)}\right] \tag{30}$$

The σ is a temperature shift in the unit of 1/T. The correlation function directly determines the activation energy of deep level.

6.3. Temperature shift operator $C_n(T\cdot p) = \mathcal{T}_p[C_n(T)]$

Let $C_n(T)$ be normalized capacitance signal at certain gate time t. Denote $L(T) = Ln[C_n(T)]$ and $M(T) = Ln[-Ln(C_n(T))]$. According to temperature T the shift operator $\mathcal{T}_p$ moves $C_n(T)$ onto $C_n(Tp)$ for a real positive multiplicative constant p: $C_n(Tp) = \mathcal{T}_p[C_n(T)]$. In the following sections $\mathcal{T}_p$ will be derived.

Shift operator of $C_n(T)$, $L_n(T)$ and $M_n(T)$

Dividing $C_n(Tp) = e^{[-t\rho(Tp)^2 e^{-\omega/(Tp)}]}$ and $C_n(T) = e^{[-t\rho T^2 e^{-\omega/T}]}$ leads to:

$$C_n(Tp) = \mathcal{T}_p[C_n(T)] = C_n(T)^{p^2 e^{[-\frac{\omega}{T}(\frac{1}{p}-1)]}} \tag{31}$$

Similarly: $$L(Tp) = \mathcal{T}_p[L(T)] = L(T)p^2 e^{[-\frac{\omega}{T}(\frac{1}{p}-1)]} \tag{32}$$

and $$M(Tp) = \mathcal{T}_p[M(T)] = M(T) + 2Lnp - \frac{\omega}{T}\left(\frac{1}{p} - 1\right) \tag{33}$$

Calculation of energy using shift operators

With $\omega = E/k$ and by (3.1.2):

$$\omega = T\left(\frac{p}{1-p}\right) Ln\left[p^2 \frac{L(T)}{\mathcal{T}_p[L(T)]}\right] \tag{34}$$

So an arbitrary shift from L(T) to L(Tp) determines a energy constant significant within this temperature shift [T→Tp]. A technique for detection and analysis of closely spaced levels by scanning ω in various temperature range is developed. We suggest to call it the 'Selective Temperature Scan Technique' (STST).

Not only ω but also ρ is detectable via shift operators. For calculation purposes we have simplified (3.2.1) to the following relations. Suppose a shift from (T_i, t_i) to (T_k, t_k) and use short notes $L_i=L(T_i)$, $L_k=L(T_k)$:

$$\omega_{ik} = \left(\frac{T_i T_k}{T_k - T_i}\right) Ln\left[\left(\frac{L_k}{L_i}\right)\left(\frac{t_i}{t_k}\right)\left(\frac{T_i}{T_k}\right)^2\right], \quad \rho_{ik} = \left[\left(\frac{t_k^{T_k}}{t_i^{T_i}}\right)\left(\frac{T_k^{T_k}}{T_i^{T_i}}\right)^2\left(\frac{(-L_i)^{T_i}}{(-L_k)^{T_k}}\right)\right]^{\frac{1}{T_i - T_k}} \tag{35}$$

In practical case we put $t_i=t_k$ and chose T_k as close as possible to T_i , i.e. T_k displaces from T_i only by one scan step. We suggest the term '*temperature beam*' to refer to the displacement $T_k - T_i$ and the term '*temperature weighting range*' for the whole scanning temperature range from T_1 to T_2. For cases where $t_i \neq t_k$ the term '*rate beam*' means $t_k - t_i$.

7. White random noise in DLTS

In general there are two kinds of noise resource: *a*) equipment precision threshold ability which produces noise in form of either temperature or frequency micro-fluctuation and *b*) white random noise which produces constant additive outputs to the signal at all temperature and frequencies. While the first kind of noise always disturbs signal exponentially, i.e. the measure of disturbance grows exponentially with increased time or temperature variable, the white random noise is statistically independent to the signal.

Here we will focus on the random noise. In general the noise filtering techniques may be considered as the correlation averaging that rely on the correlation between input and output and/or the averaging of signal over preset time period [Schwartz, 1966]. They major disadvantage is that the smooth local structure of signal within the preset time is usually removed together with the averaging process. Obviously, the peak structure of any correlation integral of signal is more widened and more smoothened than of the signal itself.

Followed are some definitions. (1) We work with a *normalized capacitance* C_n at certain temperature T defined as $C_n(t)=C_0^{-1}\times[C(t)-C_1]$, where C_0 is C(t) at t=0 and C_1 is C(t) at t=∞. For $0<t<\infty$, $C_n(t)$ always specifies $0<C_n(t)<1$, this means that $Ln(C_n)$ has definite and negative value within this range. Taking Ln on $Ln(C_n)$ is not possible but $M=Ln[-Ln(C_n)]$ has definite values. (2) The average value of a variable x defined on the probability distribution $p(\xi)$ of a random variable ξ will be denoted $\langle x \rangle_\xi$. Practically we will consider the average values of X = Exp(-E/kT) and Ln(X) according to probability distribution of emission factor $p(\varepsilon)$. Generally, the small p-s denote density function where the capital P-s mean cumulative probability.

7.1. Statistics of emission factor p(ε) in absence of noise

At each time t and fixed temperature T, the average value of emission factor ε is given by: $\langle\varepsilon\rangle = \sum_i p_i(\varepsilon)\cdot\varepsilon_i$ where $p_i(\varepsilon)$ is a statistical weight for emission factor i. To determine the density probability function $p(\varepsilon)$ we perform the calculation for all measured t:

$$\{\mathrm{Ln}\,[C_n(t)^{-1/t}]\}_t = \{\varepsilon\}_t = \langle\varepsilon\rangle \quad (36)$$

With respect to this distribution C_n reads:

$$C_n = \mathrm{Exp}[-\langle\varepsilon\rangle\cdot t] = \mathrm{Exp}[-t\cdot\textstyle\sum_i p_i(\varepsilon)\cdot\varepsilon_i] = \prod_i \mathrm{Exp}[-t\cdot p_i(\varepsilon)\cdot\varepsilon_i]$$

Denote $C_i = \mathrm{Exp}[-t\cdot p_i(\varepsilon)\cdot\varepsilon_i]$, the emission law for closely spaced deep centers becomes:

$$C_n = \textstyle\prod_i C_i \quad (37)$$

C_i may be referred to as the *partial capacitance* of deep center i in distribution $p(\varepsilon)$.

7.2. Statistics of activation energy p(E) in absence of noise

Define $X_i = \mathrm{Exp}(-E_i/kT)$ with E_i is activation energy of deep center i. We have $\mathrm{Ln}(X_i) = -E_i/kT$. Giving any probability distribution $p(\eta)$, the averages $\langle\mathrm{Ln}(X)\rangle_\eta$ and $-\langle E\rangle_\eta/kT$ must be identical. To determine the density probability function $p(\eta)$ we perform the calculation for all measured t (with respect to that $\varepsilon = \rho T^2\mathrm{Exp}(-E/kT)$ where ρ is a constant.):

$$\{\eta = \mathrm{Ln}[-t^{-1}T^{-2}\mathrm{Ln}\,C_n(t)]\}_t = \{\mathrm{Ln}(\rho) - E/kT\}_t \quad (38)$$

As seen, $p(\eta)$ does not reveal $\langle E\rangle_\eta$ directly but $\langle\mathrm{Ln}(\rho) - E/kT\rangle_\eta$. In case $\mathrm{Ln}(\rho)$ holds fixed we may suppose that:

$$\langle\mathrm{Ln}(\rho) - E/kT\rangle_\eta = \mathrm{Ln}(\rho) - \langle E/kT\rangle_\eta = \mathrm{Ln}(\rho) - \langle E\rangle_\eta/kT. \quad (39)$$

As consequence $p(E) = p(\eta)$. However, statistics (38) always produces $\langle\mathrm{Ln}(\rho) - E/kT\rangle_\eta$ not $\langle E\rangle_\eta$ in general.

7.3. Relation between p (ε) and p(E)

Suppose that (b.2) holds e.g. $p(E) = p(\eta)$. In term of $\langle E\rangle_\eta$, the average $\langle\mathrm{Ln}X\rangle_\eta$ reads:

$$\langle\mathrm{Ln}X\rangle_\eta = -\langle E\rangle_\eta/kT = -\textstyle\sum_i p_i(E)\cdot E_i/kT \quad (40)$$

Emission factor becomes $\langle\varepsilon\rangle_\eta = \rho T^2\mathrm{Exp}(\langle\mathrm{Ln}X\rangle_\eta)$. While in term of $\langle X\rangle_\varepsilon$, $\langle\varepsilon\rangle = \sum_i p_i(\varepsilon)\cdot\varepsilon_i = \rho T^2\sum_i p_i(\varepsilon)\cdot X_i = \rho T^2\langle X\rangle_\varepsilon$. Comparing these two relations leads to:

$$\mathrm{Ln}\langle X\rangle_E = \langle\mathrm{Ln}X\rangle_\eta \quad (41)$$

We use this relation to check how much $p(\varepsilon)$ and $p(E)$ differ. If they differ too much then the relation (39) may not hold for the case under investigation. The physical meaning of (39) is that the noise effecting activation energy does not influence level concentration and capture cross-section, i.e. E and $\mathrm{Ln}(\rho)$ are statistically independent.

7.4. Statistics of emission factor p(ε) in occurrence of white random noise

In occurrence of a white random noise, capacitance signal has the form:

$$C_n = \mathrm{Noise} + \mathrm{Exp}[-\langle\varepsilon\rangle\cdot t] \quad (42)$$

Re-write C_n to:

$$C_n = \mathrm{Exp}[-\langle\varepsilon\rangle\cdot t]\cdot(1 + \mathrm{Noise}/\mathrm{Exp}[-\langle\varepsilon\rangle\cdot t])$$

and put

$\mathrm{Noise} = \kappa \cdot \mathrm{Exp}[-\langle\varepsilon\rangle \cdot t] \cdot \mathrm{Exp}[-\xi \cdot t]$ (43)

where κ is constant and ξ is a random variable. We have C_n as:

$C_n = \mathrm{Exp}[-\langle\varepsilon\rangle \cdot t] \cdot (1 + \kappa \cdot \mathrm{Exp}[-\xi \cdot t])$

Denote $C_\varepsilon = \mathrm{Exp}[-\langle\varepsilon\rangle \cdot t]$, $C_\xi = (1 + \kappa \cdot \mathrm{Exp}[-\xi \cdot t])$ and $C_{\xi n} = (C_\xi - 1)/\kappa$:

$C_n = C_\varepsilon \cdot C_\xi$ or $C_n = C_\varepsilon \cdot (1 + \kappa \cdot C_{\xi n})$ (44)

This means that the capacitance transient in occurrence of noise follows relation (37) for closely spaced deep centers, e.g. random noise behaves as if it is a deep center. This would not be true if ξ does not have density probability similar to C_n . Fortunately, for arbitrary positive noise level [Noise] equation (43) always has solution $\xi = \mathrm{Ln}(\mathrm{Noise}/\kappa)^{-1/t} - \langle\varepsilon\rangle$. If [Noise] is a random noise with uniform density, than ξ has density probability of $\mathrm{Ln}(\mathrm{Noise}/\kappa)^{-1/t} - \langle\varepsilon\rangle$ which is practically the same as C_n (Fig.6).

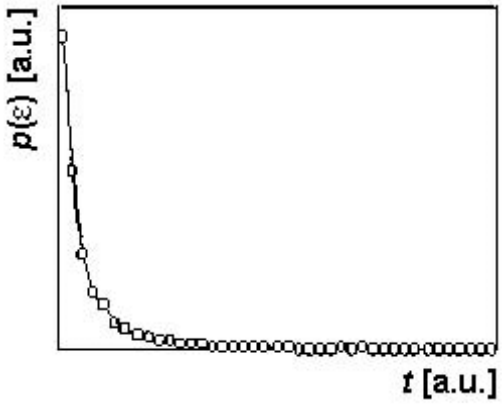

Fig.6. Density probability $p(\xi)$ of $\xi = \mathrm{Ln}(\mathrm{Noise}/\kappa)^{-1/t} - \langle\varepsilon\rangle$

Clearly, for all measured t the statistics $p(\varepsilon)$:

$\{\mathrm{Ln}(C_n)^{-1/t}\}_t = \{-\langle\varepsilon\rangle + \varepsilon_\xi\}_t$ (45)

where $\varepsilon_\xi = \{\mathrm{Ln}(1 + \kappa \cdot \mathrm{Exp}[-\xi \cdot t])^{-1/t}\}$ will reveal average value of $\{-\langle\varepsilon\rangle + \varepsilon_\xi\}$ which differs generally from (36).

Fig.7 shows $p(\varepsilon)$ for 3 different T. As seen, while at the middle T the real ε peak is high and proportional to the noise peak ε_ξ , at the high T the real ε peak is a lot smaller than the noise peak ε_ξ .The side-effect of ε_ξ is that it widens the width of a delta-like (36) peak with the amount proportional to $\langle\varepsilon_\xi\rangle$. One may expect that if $\langle\varepsilon\rangle$ and ε_ξ are absolutely additive than the distribution spectrum of (45) will contain only one smooth Gaussian peak.

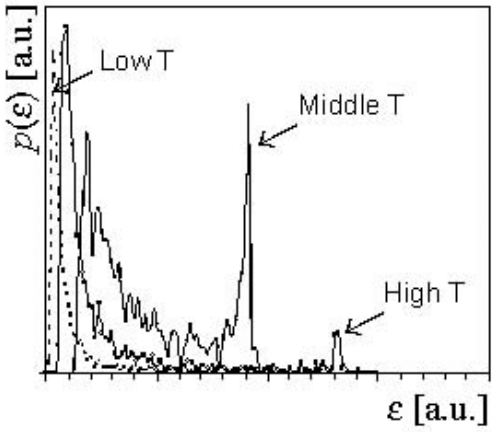

Fig.7. Spectrum $\{ \mathrm{Ln}(C_n)^{-1/t} \}_t$ at various temperature T. Noise = 2% of C_n unit.

However Fig.8 shows two different area, one corresponds to $<\varepsilon>$ and the other to ε_ξ. This is separation is true with two exceptions, the first occurs at low T when C_n is practically equal 1 and the second occurs at high T when C_n is near 0. In both cases, noise becomes so dominating that spectrum $\{ \mathrm{Ln}(C_n)^{-1/t} \}_t$ contains only values of $\{ \varepsilon_\xi \}_t$.

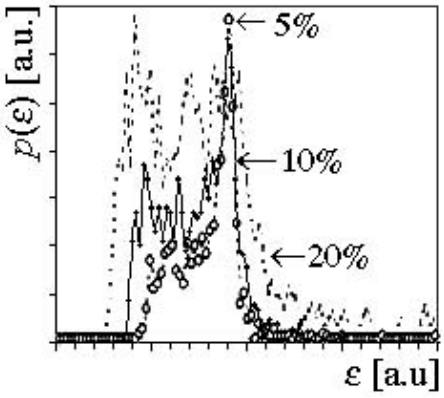

Fig.8. The existence of two different area for $<\varepsilon>$ and ε_ξ at noise level 5%, 10% and 20% of C_n unit.

8. Vibrated boxcar technique

In this section we describe a measurement system which monitors the capacitance transient signals $C(t)$ at the preset T by a variable multiplicator - a vibrating boxcar. The main idea bases on a single boxcar which instead of being fixed at certain position, vibrates with some preset frequency. If we now imagine the decreasing of the capacitance signal over time t through a region $[t-d, t+d]$ when the gate - set up before at the central position t vibrates with amplitude d, than the result C from the multiplicator circus should lie in the range $[C(t-d), C(t+d)]$ (see Fig.9). Giving t, d and by measuring C, the emission factor $e(T)$ can be deduced directly without the repeatedly scan of the temperature.

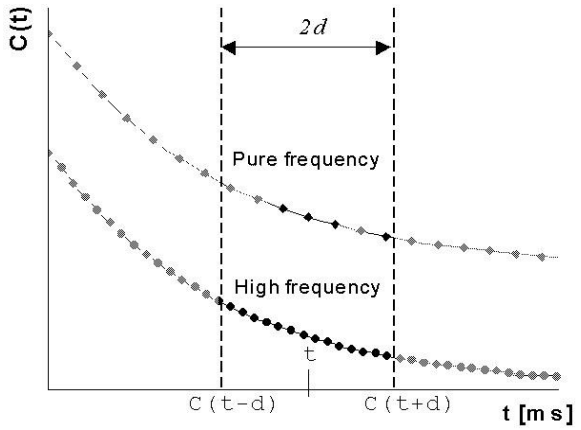

Fig.9. The occurence of the transient signals when the gate vibrates with various frequencies. When the frequency was set large enough compared to the proper relaxation time the whole band of the transient was recorded. Otherwise at the lower vibration frequency only some segments of the transient felt inside the gate vibration amplitude interval. The relation (5) is not valid in these cases.

Let `t` be a preset time around which the gate vibrates with amplitude `d` and with certain frequency `F`. When a transient signal decreases according to `t`, it crosses with the gate at some positions lain in the range [`C(t-d), C(t+d)`]. However the exact values of the occurences depend on the frequency `F`. If `F` was large enough compared to the proper relaxation time of the transient, the recorded values should fill the whole band [`C(t-d), C(t+d)`]. If `F` was comparable to the relaxation time than only several occurences should be recorded and if `F` was too small, it might happen that no point should be recorded. We will now consider only the case where the whole band [`C(t-d), C(t+d)`] is fulfilled with the transients.

In general case, the emission factor depends on temperature according to relation:

$$e = e_0 T^2 \exp(-\frac{E}{kT}) \tag{46}$$

where e_0 is a pre-factor depending on the level concentration and the capture cross section, E is the level activation energy and k is the Boltzmans constant. In term of e the capacitance transient $C(t)$ reads:

$$C(t) = C_0 + \Delta C \exp(-et) \tag{47}$$

The D.V.Lang's signal is defined as:

$$S(T) = C(t-d) - C(t+d) = \Delta C[\exp(-e(t-d)) - \exp(-e(t+d))] \tag{48}$$

Scale the $S(T)$ on ΔC and move the exp(–et) out of the brackets, we get:

$$\frac{S(T)}{\Delta C} = \exp(-et)[\exp(ed) - \frac{1}{\exp(ed)}]$$

Denote $s(T) = Ln[\frac{S(T)}{\Delta C}], \delta = Ln[\exp(ed) - \frac{1}{\exp(ed)}]$ we have finally:

$$s(T) = -et + \delta \tag{49}$$

Providing that d is preset the δ is always constant. The $s(T)$ can be obtained by setting:

$$s(T)=C_{max}-C_{min} \quad (50)$$

Note that this relation (50) holds only if the vibration frequency `F` is large enough compared to the proper relaxation time of the transients. The accuracy of the method depends wholly on the accuracy of this relation.

By varying the time *t*, the line (49) can be constructed and its slope reveals the emission factor *e* at the preset temperature `T`. So we get 1 point for the relation (46). Repeat the process after temperature `T` and construct the Arhenius plot for the determination of the activation energy `E`. This method requires only 1 temperature scan.

One of major advantage of this method is that it does not require the temperature step to be set too fine as for the other methods. In general it needs only 5 temperatures to be maintained, so the measuring time is greatly shortened. The temperature step can be set as large as the whole temperature band divided by 5. The sensitivity of this method is *strongly correlate* with the vibration frequency and fulfilling the statement (50) is not valid at the low frequency, is better at the raising frequency and is fulfilled at the frequency high enough for the case under investigation. The method is resistible to the occurrence of random noise, since the statement (50) - influenced by the statistical weight of the measured transient band [`C(t-d)-C(t+d)`], is not affected very much by the random noise.

9. Conclusion

Although many algorithms have been involved in the industrial manufacturing of the DLTS equipment such as in the Fourier BIO-RAD DL5000 systems, the development is still going on to improve further the resolution of the method. The newest studies promises more sensibility and faster measurement while providing more complex outputs and enhance the ability of the method.

Acknowledgement

This research is funded by Vietnam National Foundation for Science and Technology Development (NAFOSTED) under grant number 103.02-2017.18.

References

[1] D.V. Lang, J. Appl. Phys. 45, (1974) p.3023.

[2] de Prony, Baron Gaspard Riche (1795). Essai éxperimental et analytique: sur les lois de la dilatabilité de fluides élastique et sur celles de la force expansive de la vapeur de l'alkool, à différentes températures. *Journal de l'École Polytechnique*, Vol.1, cahier 22, 24-76.

[3] Osborne, M.R. and Smyth, G.K. (1991). A modified Prony algorithm for fitting functions defined by difference equations. *SIAM Journal of Scientific and Statistical Computing*, 12, 362-382.

[4] S. Weiss & R. Kassing, Solid State Electronics, Vol. 31, 12 (1988) p. 1733

[5] L. Dobaczewski, P. Kaczor, I.D. Hawkins, A.R.Peaker, Mat.Sci.and Tech. 11 (1994) p. 194-198.

[6] Hoang Nam Nhat & Pham Quoc Trieu, Proceedings of the VGS5 2002, p.115-119.

[7] C. Hurtes, M. Boulou, A. Mitonneau, D. Bois. Appl. Phys. Lett. 32 (1978) p.821-823.

[8] J. Morimoto, M. Fudamoto, K. Tahira, T. Kida, S. Kato, T. Miyakawa, Jap. J. Appl. Phys. 26 (10) (1987) p.1634-1640.

[9] M. Pawlowski, Rev. Sci. Instrum., 70 (1999) p. 3425-3428.

[10] M. Okuyama, H. Takakura, Y. Hamakawa, Solid-State Elect., 26 (1983) p.689-694.

[11] F.R.Shapiro, S.D.Senturia, D.Adler, J.Apply.Phys., 55 (1984) p.3453.
[12] Z. Su, J.W.Farmer, J. Apply. Phys., 68(1990), p.4068.
[13] I. Thurzo, D. Pogany, K. Gmucova, Solid-State Elect., 35 (1992) p.1737-1743.
[14] K. Ikeda, H. Takaoka, Jap.J.Appl.Phys.,21(1982) p.462-466.
[15] Hoang Nam Nhat and Pham Quoc Trieu, J. of Sciences: Mathematics - Physics, No.4, 2002, p.28-36.
[16] M. Schwartz et al., Comm. Systems & Techniques, McGraw-Hill 1966, p.63
[17] S.W. Provencher, Comp. Phys. Commun. 27, (1982) p.213
[18] W.A. Doolittle & A. Rohatgi, J. Appl. Phys. 75, (1994) p.9.